Ab initio cluster calculations of hydrogenated GaAs(001) surfaces

Q. Fu

Chemical Engineering Department, University of California, Los Angeles, California 90095-1592

L. Li

Department of Physics and Laboratory for Surface Study, University of Wisconsin, Milwaukee, Wisconsin 53201

R. F. Hicks*

Chemical Engineering Department, University of California, Los Angeles, California 90095-1592

Hydrogen adsorption on the (2×4) and (4×2) reconstructions of gallium arsenide (001) has been studied by internal reflectance infrared spectroscopy and *ab initio* cluster calculations with density-functional theory. The calculations are made on $Ga_5As_4H_{11,13}$, $Ga_4As_5H_{11,13}$, and $Ga_7As_8H_{19}$ clusters, which model the arsenic- and gallium-dimer termination of the semiconductor surface. Excellent agreement has been achieved between the vibrational frequencies predicted by the theory and those observed in experiments. On the (2×4), hydrogen adsorbs on arsenic dimers to form isolated and coupled arsenic-monohydrogen bonds, and arsenic-dihydrogen bonds. Conversely, on the (4×2), hydrogen adsorbs on gallium dimers to form terminal and bridged gallium hydrides. The latter species occur in isolated or coupled structures involving two or three Ga atoms.

I. INTRODUCTION

Vapor-phase growth processes, including metal-organic vapor-phase epitaxy (MOVPE), molecular beam epitaxy (MBE), and chemical beam epitaxy (CBE), are the techniques of choice for manufacturing III/V compound semiconductor devices. These devices have many applications, including full-spectrum light-emitting diodes, microwave devices, broadband communications, and space solar cells.[1] It is well known that the performance of a device strongly depends upon the growth process.[2] In particular, the structure and composition of the surface during epitaxy translates directly into the structure and composition of the bulk film. Therefore, a thorough understanding of the surface physics of compound semiconductors is needed to unlock the full potential of these fabrication processes.

Scanning tunneling microscopy (STM) is one of the principal methods used to investigate the surface structure of semiconductors. It yields the local density of states with atomic resolution.[3–6] Nevertheless, difficulties can arise in interpreting the STM images because the instrument folds together topographic features with electronic effects.[7] In addition, the chemical composition cannot be distinguished solely from the images. To overcome these problems, sophisticated total-energy calculations have been performed to aid in the analysis of the STM results.[5,8–11] This latter technique works well provided that the researchers have included the correct structure in their calculations.

Therefore, it is desirable to complement scanning tunneling microscopy with a chemically specific surface probe. Infrared spectroscopy of adsorbed hydrogen is well suited for this task, since hydrogen atoms titrate the dangling bonds, and the frequencies of the *M*-H stretching vibrations are very sensitive to the local chemical environment on the surface.[12–18] To help analyze the data, one can compare the infrared spectra with those obtained for gas-phase molecules.

However, this comparison is not straightforward because the structures formed on the surface do not have exact molecular analogs in the gas.

An alternative approach to interpreting vibrational spectra of surfaces is to assemble cluster models of the adsorbate complex and predict the *M*-H stretching frequencies using theoretical methods.[17,19–24] Chabal and Raghavachari have applied this technique to hydrogen-terminated silicon. They examined the clusters Si_3H_8 and Si_9H_{14}, and by comparison to their experimental data, found that coupled silicon monohydrides H-Si-Si-H and to a lesser extent, silicon dihydrides (H-Si-H) are formed on the (100) and (111) surfaces.[17] These authors also have applied these methods to the study of the initial oxidation of Si (100).[19,20] Another example of combining vibrational spectroscopy with cluster calculations is provided in the work of Shan, Wang, and Hamers[21] on phosphine adsorption on Si(100).

We have investigated gallium arsenide and indium phosphide (001) using scanning tunneling microscopy and infrared spectroscopy of adsorbed hydrogen.[12–16] These surfaces are terminated with group III and V dimers. Hydrogen bonds to the dimer atoms, producing a series of vibrational bands due to gallium hydrides ($1900–1000$ cm^{-1}), indium hydrides ($1650–1000$ cm^1), arsenic-hydrogen species ($2150–2000$ cm^{-1}), and phosphorus-hydrogen species ($2350–2200$ cm^{-1}). On GaAs(001) there are also missing dimer rows, which lead to hydrogen adsorption onto second-layer arsenic and gallium atoms. The large number of vibrational bands observed on these surfaces indicates that hydrogen forms a variety of different chemical bonds to the exposed atoms. As of yet, it has not been possible to conclusively assign the infrared peaks to specific adsorbate structures.

In this paper we report on a comprehensive study of the molecular structure of gallium arsenide clusters: $Ga_5As_4H_{11,13}$, $Ga_4As_5H_{11,13}$, and $Ga_7As_8H_{19}$. These clusters provide an accurate model of hydrogen adsorption on the

TABLE I. Vibrational modes observed for the hydrogen-terminated (2×4) surface as determined by theory and experiment.

Assignment	Theory Frequency (cm^{-1})	Intensity	Cluster [a]	Experiment Frequency (cm^{1})	Intensity
H_4-As_2-H_5 [b]	2150	m	2	2138	m
H_4-As_2-H_5 [c]	2118	s	2	2109	s
H_3-As_1As_2-H_4 [c]	2118	s	1		
H_3-As_1As_2-H_4 [b]	2106	w	1		
:As_1-H_3	2024	m	2	2025	m
H_3-As_1::As_2-H_4 [c]	2007	w	3		
H_3-As_1::As_2-H_4 [b]	2000	s	3	2000	s
(As)Ga-H	1834	m	6	1835	m

[a]Refer to Fig. 2.
[b]Asymmetric.
[c]Symmetric.

gallium and arsenic dimers exposed on the GaAs(001) surface. Moreover, the vibrational properties of these clusters are in excellent agreement with the infrared spectra recorded of adsorbed hydrogen on the (2×4) and (4×2) reconstructions of gallium arsenide. We show that the vibrational data are adequately explained by a series of coupled and isolated arsenic-monohydrogen bonds, arsenic-dihydrogen bonds, terminal gallium hydrides, and isolated and coupled bridging gallium hydrides.

II. EXPERIMENTAL METHODS

The samples were prepared by growing GaAs films, 0.5-μm thick, on gallium arsenide (001) substrates in a metal-organic vapor-phase epitaxy (MOVPE) reactor.[14] After growth, samples were transferred directly into an ultra-high vacuum (UHV) chamber that was held at a base pressure of 2.0×10^{-10} Torr. Then, the (2×4) and (4×2) reconstructions were obtained by annealing the crystals at 450 °C and 520 °C, respectively. The reconstructions were characterized by low-energy electron diffraction, x-ray photoelectron spectroscopy, and scanning tunneling microscopy.[6,14]

The infrared spectra were obtained by multiple internal reflection through GaAs (001) crystals that were 10-mm wide by 40-mm long by 0.64-mm thick, and with 45° bevels at each end. A total of 31 reflections occurred off the front face of the crystals. Two substrate orientations were used: one with the long crystal axis parallel to the [$\bar{1}$10] direction, and one with the long crystal axis parallel to the [110] direction. Hydrogen was dosed into the chamber at 5×10^{-7} Torr, and dissociated with a tungsten filament located 4 cm from the sample face. Dosing was continued for 30 min (900 L H_2) to allow the hydrogen atoms to saturate the exposed sites on the semiconductor surface. A series of infrared spectra were collected before and during this exposure, using a Diglab FTS-40A Fourier-transform infrared spectrometer. The spectra were recorded at 8-cm^{-1} resolution and coadding 1024 scans. The vibrational bands observed in the reflectance spectra are summarized in Tables I and II for the (2×4) and (4×2) surfaces, respectively. It should be noted that heating the samples to 300 °C desorbs the hydrogen and

regenerates the (2×4) and (4×2) reconstructions, as observed by low-energy electron diffraction.

III. THEORETICAL METHODS

Ball-and-stick models of the arsenic-rich (2×4) and gallium-rich (4×2) reconstructions are shown in Fig. 1. These two structures are the most studied surface phases of gallium arsenide.[3–6] On the $\beta 2(2 \times 4)$, the uppermost layer is terminated with two rows of arsenic dimers extending along the [$\bar{1}$10] crystal direction. These rows are separated by a trench that is terminated with a single row of arsenic dimers. Theoretical and experimental studies of the $\beta 2(2 \times 4)$ have shown that the dangling bonds on the As dimers are filled with lone pairs of electrons, while the dangling bonds on the threefold coordinated Ga atoms in the second layer are empty.[25–27] A molecular cluster, having the minimum size required to simulate this surface structure, is highlighted with gray and black spheres in Fig. 1(a). This cluster contains a single arsenic dimer tethered to five ''bulk'' Ga atoms and two ''bulk'' As atoms, and has the molecular formula, $Ga_5As_4H_9$. Ten hydrogen atoms are bonded to the As and Ga atoms to avoid spin and charge contamination that would result from truncation of the Ga-As bonds. Furthermore, the number of H atoms is chosen so that the number of nonbonding electrons equals twice the number of threefold coordinated As atoms.

The (4×2) surface exhibits the same structure as the (2×4), except that it is terminated with rows of gallium dimers extending in the [110] crystal direction. Two molecular clusters have been constructed to simulate this surface, $Ga_4As_5H_9$ and $Ga_7As_8H_{17}$ (highlighted black and gray spheres in Figs. 1(b) and 1(c). These structures contain two and three surface Ga atoms, and as discussed below, serve as templates for the formation of isolated and coupled bridging gallium hydrides.

By bonding different numbers of hydrogen atoms to the threefold coordinated As and Ga atoms on the clusters, we created nine distinct $Ga_xAs_yH_z$ molecules. Only six could be optimized by *ab initio* molecular-orbital calculations, and these are presented in Fig. 2. They consist of $Ga_5As_4H_{13}$ (1 and 2), $Ga_5As_4H_{11}$ (3), $Ga_4As_5H_{13}$ (4), $Ga_4As_5H_{11}$ (5), and $Ga_7As_8H_{19}$ (6). Hydrogen is bonded to the ''surface'' atoms

TABLE II. Vibrational modes observed for the hydrogen-terminated (4×2) surface as determined by theory and experiment.

Assignment	Theory			Experiment	
	Frequency (cm^{-1})	Intensity	Cluster [a]	Frequency (cm^{-1})	Intensity
Ga_1-H_3	1880	m	5	1878	m
Ga_1-H_3 [b]	1869	m	4		
Ga_1-H_3 [c]	1866	w	4		
Ga_1-H_3	1862	m	6		
Ga_1-H_4-Ga_2 [c]	1725	s	4	1729	s
Ga_1-H_4-Ga_2 [c]	1637	s	5	1604	s
Ga_1-H_4-Ga_2-H_5-Ga_6 [c]	1532	s	6	1481	s
Ga_1-H_4-Ga_2-H_5-Ga_6 [b]	1549	w	6		
Ga_1-H_4-Ga_2 [b]	775	w	4		
Ga_1-H_4-Ga_2 [b]	747	w	5		
Ga_1-H_4-Ga_2-H_5-Ga_6 [d]	756	w	6		
Ga_1-H_4-Ga_2-H_s-Ga_6 [e]	705	w	6		
$(3Ga)As_8$-H	2073	s	6	2078	s
				2050	s

[a]Refer to Fig. 2.
[b]Symmetric.
[c]Asymmetric.
[d]Rocking.
[e]Scissors.

(numbered 1, 2, and 6 in the figure) in as many ways as possible to simulate the types of M-H bonds that can form on GaAs(001). In the six optimized clusters, each arsenic dangling bond is filled with a pair of electrons, while each gallium dangling bond is empty. The clusters that could to be optimized contained either too many or too few electrons to achieve filled As and empty Ga dangling-bond states. This result is consistent with the electron-counting model that has been established for GaAs(001) reconstructions.[27]

The GAUSSIAN98 quantum chemistry suite was used to compute the structure of each $Ga_xAs_yH_z$ molecule.[28] The electron correlation effect was assessed with Perdew-Wang's gradient-corrected correlation and exchange functionals, dubbed PW91PW91.[29] Stuttgart-Dresden's relativistic pseudopotentials (SD-ECP) were employed for the Ga and As core electrons,[30] while the valence electrons were treated with $(4s,4p)/[2s,2p]$ contracted basis sets.[31] For hydrogen, the Dunning-Huzinaga valence double-ζ basis set was selected.[32] During closed-shell energy minimization, all the atoms were allowed to fully relax to their optimal positions. Then the vibrational frequencies were determined by taking the second derivative of the energy with respect to the Cartesian coordinates of the nuclei. No imaginary frequencies were obtained for the six clusters presented in Fig. 2.

To evaluate the accuracy of the calculations, we determined the M-H stretching frequencies of AsH_3 and Ga_2H_6 molecules with larger basis sets, like Pople's triple split, with polarization. It was found that the PW91PW91 with SD-ECP yielded essentially the same values as the larger basis sets, but with less computing time. For example, two infrared bands have been recorded for arsine at 2123 and 1003 cm^{-1}.[33] The theoretical methods yield 2091 and 1014 cm^{-1} by SD-ECP, and 2162 and 991 cm^{-1} by the 6–311G** basis set. For digallane, the asymmetric stretch for bridging gallium hydride is located at 1273 cm^{-1}.[34] Our calculations yield 1256 and 1306 cm^{-1} using the SD-ECP and 6-311 G** basis sets, respectively. Below, the predicted
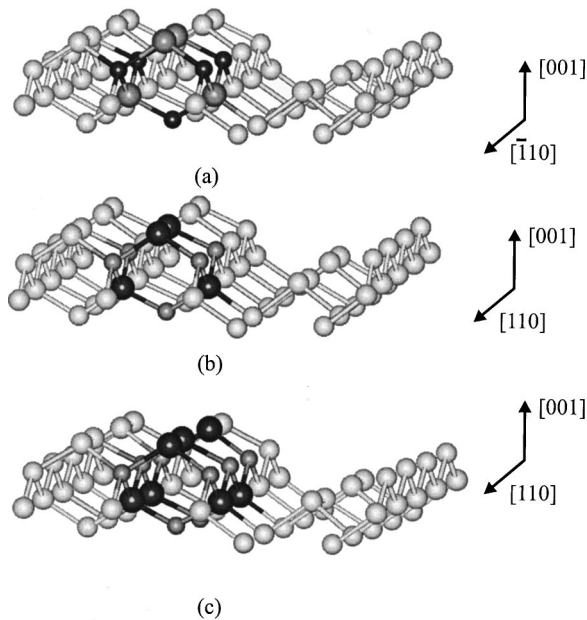

FIG. 1. Perspective view of the GaAs(001) surface: (a) (2×4), (b) and (c) (4×2). The gray and black spheres highlight the GaAs clusters used in the calculations: (a) Ga_5As_4, (b) Ga_4As_5, and (c) Ga_7As_8. The gray and black spheres are arsenic and gallium atoms, respectively, while the white spheres are for the rest of arsenic and gallium atoms.

1. Ga$_5$As$_4$H$_{13}$

2. Ga$_5$As$_4$H$_{13}$

3. Ga$_5$As$_4$H$_{11}$

4. Ga$_4$As$_5$H$_{13}$

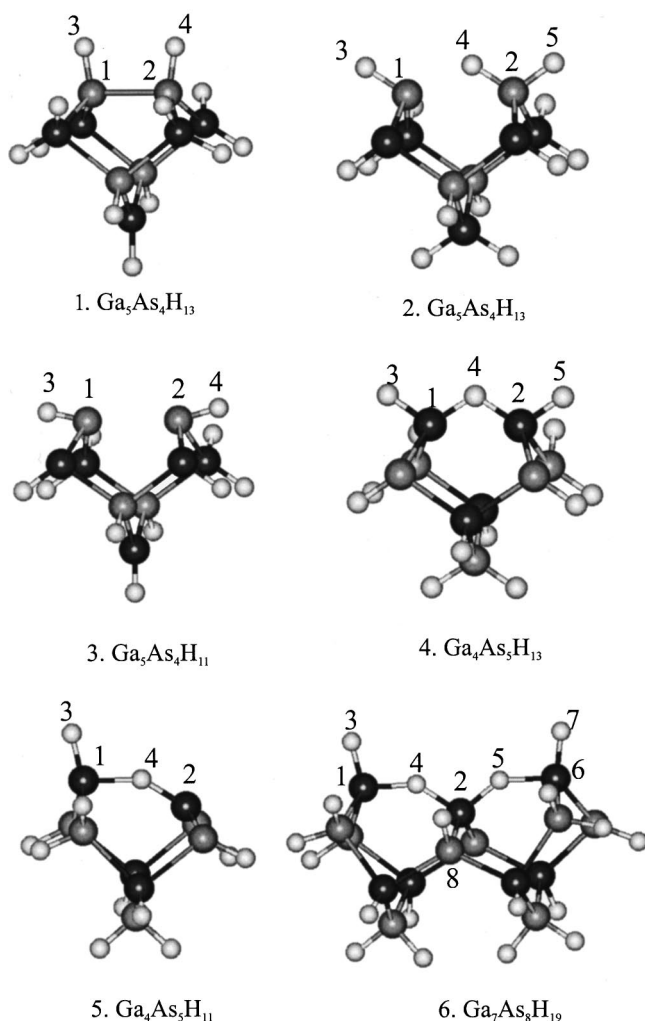5. Ga$_4$As$_5$H$_{11}$

6. Ga$_7$As$_8$H$_{19}$

FIG. 2. Ball-and-stick models of the optimized clusters, showing arsenic-hydrogen bonds (1–3) and gallium-hydrogen bonds (4–6). The As, Ga, and H atoms are the large gray, large black and small white spheres, respectively.

As-H stretching frequencies are reported without adjustment, while the predicted Ga-H stretching frequencies have been shifted upwards by 70 cm^{-1}. Frequency scaling is often employed to compensate for systematic error introduced by the computations.[18,35]

IV. RESULTS AND DISCUSSION

A. Arsenic-rich (2×4) surface

Clusters 1, 2, and 3 in Fig. 2 show four different ways in which hydrogen atoms may bond to arsenic dimers on the (2×4) surface. They may add to each dangling bond, forming a coupled H-As-As-H species as in 1, or they may insert into the arsenic dimer bond, thereby producing isolated: As-H and coupled H-As::As-H species as in 2 and 3. In addition, hydrogen may attack both sides of an arsenic dimer, generating a dihydrogen bond as in 2. The vibrational modes predicted for each of these structures are listed in Table I. Also shown in the table are the frequencies and intensities of the infrared bands observed for hydrogen adsorption on the (2×4) reconstruction.[12–14] Note that excellent agreement is achieved between the theory and the experiment.

The arsine dihydrogen bond exhibits asymmetric and symmetric stretching vibrations at 2150 and 2118 cm^{-1}. The asymmetric stretch is of moderate intensity and produces a dipole moment parallel to the arsenic dimer bond (i.e., the [110] crystal axis). On the other hand, the symmetric stretch shows strong intensity and has a dipole moment perpendicular to the surface plane. These modes correspond closely to the bands recorded at 2138 and 2109 cm^{-1} on the hydrogen-terminated (2×4) surface. Moreover, measurements made with polarized infrared light, reflected internally through GaAs(001) crystals oriented along the [$\bar{1}$10] and [110] directions, are in good agreement with the predicted dipole moments. For example, if the infrared beam travels parallel to the [110] axis, the peak at 2138 cm^{-1} is relatively intense in the *s*-polarized spectrum. Conversely, if the beam travels parallel to the [$\bar{1}$10] axis, no peak at 2138 cm^{-1} is detected with *s* polarization.[14]

The coupled arsenic-monohydrogen bond (H-As-As-H) is calculated to have an intense symmetric stretch at 2118 cm^{-1} and a weak asymmetric stretch at 2106 cm^{-1}. The former mode overlaps directly with the symmetric stretch of AsH$_2$. These results are consistent with the experimental measurements, wherein a single peak is detected at 2109 cm^{-1}, having a strong *p*-polarization irrespective of the crystal orientation. It is interesting to note that for AsH$_2$, the asymmetric mode vibrates at a higher frequency than the symmetric mode, while the opposite is true for H-As-As-H. Similar results have been reported on hydrogen-terminated Si(100) by Chabal.[18] He attributed this to the difference between local dynamical coupling, i.e., chemical shifts, and inter-unit-cell dynamical coupling.

Hydrogen bonded to an arsenic atom with a pair of electrons in its dangling bond may exhibit an isolated stretching vibration (:As-H) as in cluster 2 (Fig. 2), or a coupled stretching vibration (H-As::As-H) as in cluster 3. The isolated and coupled modes are predicted to yield two intense peaks at 2024 and 2000 cm^{-1}. These assignments are in excellent agreement with the observed infrared bands at 2025 and 2000 cm^{-1} on the hydrogen-terminated (2×4) surface. Moreover, the theory indicates that these modes produce a dipole moment nearly parallel to the [$\bar{1}$10] crystal axis, which is consistent with the polarization dependence observed for these infrared bands. The weak dynamic coupling between the two :As-H species in cluster 3 produces a split of only 7 cm^{-1} between the symmetric and asymmetric modes, and the former vibration at 2007 cm^{-1} is of very low intensity. A peak corresponding to this symmetric mode could not be identified in the experimental infrared spectra.

Examination of the (2×4) model in Fig. 1 reveals that second-layer gallium atoms are exposed along each edge of the trench. Hydrogen atoms can coordinate to the dangling bonds of these Ga atoms and produce an isolated Ga-H stretching vibration. As shown in Table I, the theory predicts that a gallium atom bonded to three arsenic atoms and one hydrogen atom will yield a single Ga-H peak at 1834 cm^{-1}. In experiments on the (2×4) surface, we have recorded two gallium hydride bands at 1878 and 1835 cm^{-1}, with polarization consistent with the dipole moments being oriented along [110] direction. During H-atom dosing, the former band grows in after the latter one has reached its maximum

TABLE III. Bond lengths and bond angles of the three arsenic-rich clusters (bond length is in angstroms).

Parameters	Cluster type 1	Cluster type 2	Cluster type 3
$As_1 \cdots As_2$	2.534	4.214	3.874
As_2-H_4	1.536	1.527	1.562
As_2-H_5		1.531	
As_1-H_3	1.536	1.563	1.562
$\angle H_3$-$As_1 \cdots As_2$	99.4°	1.78.0°	178.3°
$\angle H_4$-As_2-H_5		98.1°	

intensity.[13] The most likely explanation for the appearance of the 1878 cm^{-1} peak is that some etching of the top-layer As atoms occurs during dosing.

Listed in Table III are some of the bond lengths and bond angles obtained for the optimized clusters 1, 2, and 3. Before hydrogen adsorption, we calculate an arsenic dimer bond length of 2.564 Å. Adsorption of hydrogen onto the ends of the arsenic dimer, as in 1, causes the As-As bond to shorten to 2.534 Å. This shortening is attributed to the higher coordination about the arsenic atom and the addition of more s character to the molecular orbitals.[36,37] The mixing of s and p atomic orbitals on the fourfold-coordinated As atom is also evident in the As_1-H_3 bond length of 1.536 Å. These results may be contrasted to the arsenic monohydrogen bonds on clusters 2 and 3, where a lone pair of electrons remains in the dangling bond. In this case, the As_1-H_3 bond length is longer, 1.563 Å. The lone pair of electrons, which mainly populates the unmixed 4s orbital, effectively screens the arsenic nucleus from the hydrogen atom. The $\angle H_3$-As_1-As_2 bond angle of 178° puts the As-H bond at nearly a right angle to the Ga-As back bonds, as expected for the use of predominately 4p orbitals in bond formation.

B. Ga-rich (4×2)

Clusters 4, 5, and 6 in Fig. 2 represent the different ways in which hydrogen may bond to gallium dimers on the (4×2) reconstruction. The H atoms may adsorb onto a dangling orbital, forming a terminal gallium hydride (Ga_1-H_3), or they may insert into the dimer bond, forming a bridging gallium hydride (Ga_1-H_4-Ga_2). In cluster 6, two bridging hydrides are shared between three gallium atoms. This results in coupling of the vibrational modes.

The vibrational properties of the gallium hydride bonds are summarized in Table II. In addition, the predicted infrared bands are compared to those recorded following hydrogen adsorption of the (4×2) surface.[14] According to the theory, the two terminal hydrides on cluster 4 exhibit coupling with a symmetric mode at 1869 cm^{-1} and an asymmetric mode at 1866 cm^{-1}. The peak intensity of the former vibration is predicted to be much greater than the latter. In addition, the symmetric mode should yield an infrared peak that is strictly p-polarized regardless of the crystal orientation, since the dipole moment is perpendicular to the surface. Examination of our experimental infrared spectra does not reveal a band with these properties. The peak observed at 1878 cm^{-1} is predominantly s-polarized when the GaAs internal reflection element is cut parallel to the [$\bar{1}$10] axis. The

predicted band at 1869 cm^{-1} is not detected for two reasons: first, its population is limited, since an extra electron is required to form the structure that is not contributed by H-atom adsorption; and second, the intensity of this mode is reduced by dielectric screening (see discussion below).[18]

On cluster 5, hydrogen coordinates to only one end of the gallium dimer, leaving an empty orbital on the other Ga atom (refer to Fig. 2). The isolated Ga-H stretch for this bond occurs at 1880 cm^{-1}, which is essentially the same frequency as the observed infrared band at 1878 cm^{-1}. The dipole moment for this harmonic oscillator has components parallel to the [001] and [110] directions. Due to dielectric screening of the adsorbed layer perpendicular to the surface, the measured intensity along the [001] is reduced relative to that along the [110]. This is consistent with our measurements of the infrared peak at 1878 cm^{-1}: it is p polarized when the reflected light travels along the [110] crystal axis, while it is about equally s- and p-polarized when the light travels down the [$\bar{1}$10] axis.[14] Cluster 6 also contains terminal gallium hydrides. Their vibrational properties are basically the same as the terminal Ga-H bond on cluster 5, except that the frequency of the oscillation is shifted down by 18 cm^{-1}.

Hydrogen insertion into the gallium dimer bond produces a bridging gallium hydride. This species exhibits an intense asymmetric stretching mode that is parallel to the [110] crystal axis and a very weak symmetric mode that is normal to the surface. As shown in Table II, the asymmetric stretching vibrations for the bridging hydrides on clusters 4 and 5 are predicted to be at 1725 and 1637 cm^{-1}, respectively. These values are in good agreement with the infrared spectra for hydrogen adsorption on the (4×2) surface, which contain intense broad bands at 1729 and 1604 cm^{-1}. In addition, the polarization of these bands indicates that the vibrations are parallel to the [110] direction. The weak symmetric vibrations for the bridging hydrides occur at 775 and 747 cm^{-1}, which falls below the absorption cutoff of 850 cm^{-1} for the GaAs crystal, and cannot be observed by experiment.

The coupled bridging hydrides on cluster 6 exhibit an asymmetric and a symmetric mode at 1532 and 1549 cm^{-1}. The former mode has a dipole moment change along [110] direction, which is in good agreement with the observed band at 1481 cm^{-1}. Conversely, the latter mode with dipole moment change along [001] direction is very weak in intensity, which cannot be observed experimentally. It also should be noted that the coupled bridging hydrides produce rocking and scissors modes of low intensity at 756 and 705 cm^{-1}.

The gallium-rich (4×2) surface contains exposed second-layer arsenic that may coordinate with hydrogen. As shown in Figs. 1(b) and 1(c), these sites occur along the edges of the trenches, and each arsenic atom is bonded to three gallium atoms (one on a dimer and two in the bulk). This site is best simulated by one of the arsenic atoms located below the center gallium atom in cluster 6 (i.e., As_8 beneath Ga_2 in Fig. 2). The predicted vibrational frequency of this species is 2073 cm^{-1}. Our infrared spectra of the hydrogen-terminated (4×2) contain two bands at 2078 and 2050 cm^{-1} due to As-H stretching vibrations.[14] The second peak could be due to coupling between adjacent species, or to a different exposed arsenic site, such as might occur at a step, or at a defect.

TABLE IV. Bond lengths and bond angles of the three gallium-rich clusters (bond length in angstroms).

Parameters	Clusters		
	4	5	6
Ga_1-Ga_2	3.502	3.462	3.381
Ga_1-H_3	1.596	1.591	1.596
Ga_1-H_4	1.771	1.881	1.854
Ga_2-H_4	1.771	1.731	1.746
$\angle H_3$-Ga_1-H_4	102.9°	103.2°	98.2°
$\angle Ga_1$-H_4-Ga_2	162.8°	155.8°	139.8°
$\angle Ga_1$-Ga_2-Ga_6			145.9°

Some of the structural properties of the optimized clusters 4, 5, and 6 are presented in Table IV. The gallium-gallium bond distances for these three molecules decreases from 3.502 to 3.462 to 3.381 Å , respectively, indicating that each successive bridging hydride is more stable than the preceding one. The fact that the trimer is lower in energy than the dimer is consistent with previous work. Duke, Liang, and Schaefer have shown theoretically that trimers (M_3H_9) are energetically preferred over dimers (M_2H_6).[38] In an experimental study, Pulham *et al.*[34] found that digallane molecules trapped in liquid nitrogen oligomerize upon heating from 20 to 35 K. On the gallium-rich GaAs(001) surface [cf. Fig. 1(c)], the extended rows of gallium dimers provide a template for forming hydrogen-bridged trimers. Higher-order structures are not allowed because of the 4-Å lattice spacing. Note that on cluster 5, the gallium dimer is buckled with the fourfold-coordinated atom (Ga_1) pushed up by 0.638 Å relative to the threefold-coordinated atom (Ga_2). In this structure, Ga_2 is stabilized in a planar configuration with respect to the bulk As and H atoms. On the other hand, Ga_1 exhibits tetrahedral bonding as evidenced by the H_3-Ga_1-H_4 bond angle of 103.2°.

According to valence-force theory, the asymmetric and symmetric stretching modes of the bridging hydride can be related to one another through the bond angle θ by Eq. (1),[39,40]

$$\nu_{as}/\nu_s = \tan(\theta/2). \tag{1}$$

This equation holds provided the angle is close to 90° so that the force constant for *M*-H bending is negligible. As shown in Table V, the approximation works well for the digallane molecule, where θ equals 95.6°. However, at the larger angles found in clusters 4 and 5, the frequency ratio is significantly lower than $\tan(\theta/2)$. These results agree with previous studies of bridging hydrogen bonds in metal hydride clusters.[40] The large Ga_1-H_4-Ga_2 bond angles observed for hydrogen insertion into the gallium dimers on GaAs(001) are

TABLE V. Comparison of frequency ratio with $\tan(\theta/2)$.

Compound	ν_{As}/ν_s	θ	$\tan(\theta/2)$
Ga_2H_6 [a]	1.05	95.6°	1.09
Cluster 5	2.19	1.55.8°	4.61
Cluster 4	2.23	162.8°	6.60

[a]Reference 34.

due to the Ga-As back bonds, which try to pull the Ga atoms back to their bulk lattice positions (a=4 Å).

C. Dielectric screening

In our studies of hydrogen adsorption on GaAs (001), we have found that the intensity of the *p*-polarized infrared bands is usually lower than that of the *s*-polarized bands. This is due to the dielectric screening effect as pointed out by Chabal.[18] According to a three-layer model, the perpendicular mode is subject to dielectric screening with a factor of $\varepsilon_{i\infty}^2$ for the internal reflection configuration, where $\varepsilon_{i\infty}$ is the dielectric constant of the adsorbate layer. The value for the adsorbate layer is different from that of bulk GaAs, where $\varepsilon_{i\infty}^0 = 13.0$.[41] We can estimate the dielectric constant of the adsorbate based on the structures obtained from *ab initio* calculations. The best mode to use for this calculation is the stretching vibration of the As_8-H bond on cluster 6, since it is straightforward to relate the theory to the experimental results. The As-H bond on this cluster is oriented 42° to the surface normal. A comparison of the theoretical intensity ratio for *p*- and *s*-polarization I_p/I_s to the measured value, yields an adsorbate dielectric constant of 1.5. This number is in the same range for hydrogen on Si (100),[42] as expected since the bulk dielectric constants of silicon and gallium arsenide are nearly equal, 12.7 versus 13.0.[41]

V. CONCLUSIONS

In summary, we have studied hydrogen adsorption on GaAs(001) by vibrational spectroscopy and *ab initio* molecular cluster calculations. With the aid of the theory, we have made detailed assignments of the *M*-H stretching modes for each of the bands observed in the infrared spectra. This work demonstrates that the clusters $Ga_5As_4H_9$, $Ga_4As_5H_9$, and $Ga_7As_8H_{17}$ are appropriate representations of the arsenic- and gallium-rich reconstructions. When used in conjunction with experimental measurements, these models can help identify the surface chemistry of gallium arsenide.

ACKNOWLEDGMENTS

---

*Author to whom all correspondence should be addressed. Electronic address: rhicks@ucla.edu

[1]T. Whitaker and M. Meyer, Compd. Semicond. **5**, 23 (1999).

[2]G. B. Stringfellow, *Organometallic Vapor-Phase Epitaxy: Theory and Practice* (Academic Press, San Diego, 1989), p. 200.

[3]D. K. Biegelsen, R. D. Bringans, J. E. Northrup, and L. E. Swartz,

Phys. Rev. B **41**, 5701 (1990).

[4]C. B. Duke, Surf. Sci. **66**, 543 (1993).

[5]Q. K. Xue, T. Hashizume, J. M. Zhou, T. Sakata, T. Sukurai, and T. Ohno, Phys. Rev. Lett. **74**, 3177 (1995).

[6]L. Li, B. Han, S. Gan, H. Qi, and R. F. Hicks, Surf. Sci. **398**, 386 (1998).

[7] J. Tersoff and N. D. Lang, in *Scanning Tunneling Microscopy*, edited by J. A. Stroscio and W. J. Kaiser (Academic Press, San Diego, 1993), p. 11.

[8] S. B. Zhang and A. Zunger, Phys. Rev. Lett. **77**, 119 (1996).

[9] W. G. Schmidt, Appl. Phys. A: Mater. Sci. Process. **65**, 581 (1997).

[10] J. E. Northrup and S. Froyen, Phys. Rev. Lett. **71**, 2276 (1993).

[11] J. E. Northrup and S. Froyen, Phys. Rev. B **50**, 2015 (1994).

[12] H. Qi, P. E. Gee, and R. F. Hicks, Phys. Rev. Lett. **72**, 250 (1994).

[13] H. Qi, P. E. Gee, T. Nguyen, and R. F. Hicks, Surf. Sci. **323**, 6 (1995).

[14] R. F. Hicks, H. Qi, Q. Fu, B.-K. Han, and L. Li, J. Chem. Phys. **110**, 10 498 (1999).

[15] L. Li, B.-K. Han, Q. Fu, and R. F. Hicks, Phys. Rev. Lett. **82**, 1879 (1999).

[16] Q. Fu. L. Li, C. H. Li, and R. F. Hicks (unpublished).

[17] Y. J. Chabal and K. Raghavachari, Phys. Rev. Lett. **53**, 282 (1984); **54**, 1055 (1985).

[18] Y. J. Chabal, Surf. Sci. Rep. **8**, 211 (1988) and references therein.

[19] B. B. Stefanov and K. Raghavachari, Surf. Sci. **389**, L1159 (1997).

[20] J. Eng, K. Raghavachari, L. M. Struck, Y. J. Chabal, B. E. Bent, M. M. Banaszak-Holl, F. R. McFeely, A. M. Michaels, G. W. Flynn, S. B. Christman, E. E. Chaban, G. P. Williams, K. Radermacher, and S. Mantl, J. Chem. Phys. **108**, 8680 (1998).

[21] J. Shan, Y. Wang, and R. J. Hamers, J. Phys. Chem. **100**, 4961 (1996).

[22] Y. Miyamoto and S. Nonoyama, Phys. Rev. B **46**, 6915 (1992).

[23] G. Brocks, P. J. Kelly, and R. Car, Phys. Rev. Lett. **66**, 1729 (1991).

[24] L. G. LePage, M. Alouani, D. L. Dorsey, J. W. Wilkins, and P. E. Blöchl, Phys. Rev. B **58**, 1499 (1998).

[25] D. J. Chadi, Phys. Rev. Lett. **41**, 1062 (1978).

[26] W. A. Harrison, J. Vac. Sci. Technol. **16**, 1492 (1979).

[27] M. D. Pashley, Phys. Rev. B **40**, 10 481 (1989).

[28] GAUSSIAN98 (Rev. A.6), M. J. Frisch, G. W. Trucks, H. B. Schlegel, G. E. Scuseria, M. A. Robb, J. R. Cheeseman, V. G. Zakrzewski, J. A. Montgomery, R. E. Stratmann, J. C. Bruant, S. Dapprich, J. M. Millam, A. D. Daniels, K. N. Kudin, M. C. Strain, O. Farkas, J. Tomasi, V. Barone, M. Cossi, R. Cammi, B. Mennucci, C. Pomelli, C. Adamo, S. Clifford, J. Ochterski, G. A. Petersson, P. Y. Ayala, Q. Cui, K. Morokuma, D. K. Malick, A. D. Rabuck, K. Raghavachari, J. B. Foresman, J. Cioslowski, J. V. Ortiz, B. B. Stefanov, G. Liu, A. Liashenko, P. Piskorz, I. Komaromi, R. Gomperts, R. L. Martin, D. J. Fox, T. Keith, M. A. Al-Laham, C. Y. Peng, A. Nanayakkara, C. Gonzalez, M. Challacombe, P. M. W. Gill, B. G. Johnson, W. Chen, M. W. Wong, J. L. Andres, M. Head-Gordon, E. S. Replogle, and J. A. Pople, Gaussian, Inc., Pittsburgh, PA, 1998.

[29] J. P. Perdew, K. Burke, and Y. Wang, Phys. Rev. B **54**, 16 533 (1996).

[30] G. Igel-Mann, H. Stoll, and H. Preuss, Mol. Phys. **65**, 1321 (1988).

[31] A. Bergner, M. Dolg, W. Kuechle, H. Stoll, and H. Preuss, Mol. Phys. **80**, 1431 (1993).

[32] T. H. Dunning, Jr. and P. J. Hay, in *Modern Theoretical Chemistry*, edited by H. F. Schaefer III (Plenum, New York, 1976), Vol. 3, p. 1.

[33] J. Nishizawa and T. Kurabayashi, J. Electrochem. Soc. **130**, 413 (1983).

[34] C. R. Pulham, A. J. Downs, M. J. Goode, D. W. H. Rankin, and H. E. Robertson, J. Am. Chem. Soc. **113**, 5149 (1991).

[35] J. B. Foresman and Æ. Frisch, *Exploring Chemistry with Electronic Structure Methods*, 2nd ed. (Gaussian Inc., Pittsburgh, 1996), p. 64.

[36] C. Xu, K. P. Caffey, J. S. Burnham, S. H. Goss, B. J. Garrison, and N. Winograd, Phys. Rev. B **45**, 6776 (1992).

[37] D. J. Frankel, C. Yu, J. P. Harbison, and H. H. Farrell, J. Vac. Sci. Technol. B **5**, 1114 (1987).

[38] B. J. Duke, C. Liang, and H. F. Schaefer, J. Am. Chem. Soc. **113**, 2884 (1991).

[39] G. Herzberg, *Molecular Spectra and Molecular Structure, Infrared and Raman Spectra of Polyatomic Molecules* (Van Nostrand Reinhold, New York, 1945), Vol 2, p. 168.

[40] M. W. Howard, U. A. Jayasooriya, S. F. A. Kettle, D. B. Powell, and N. Sheppard, J. Chem. Soc. Chem. Commun. 18 (1979).

[41] C. Kittel, *Introduction to Solid State Physics* (Wiley, New York, 1996).

[42] Y. J. Chabal, E. E. Chaban, and S. B. Christman, J. Electron Spectrosc. Relat. Phenom. **29**, 35 (1983); Y. J. Chabal, Phys. Rev. B **29**, 3677 (1984); P. Jakob and Y. J. Chabal, J. Chem. Phys. **95**, 2897 (1991).